Chemical Science

ROYAL SOCIETY OF CHEMISTRY

EDGE ARTICLE

View Article Online
View Journal | View Issue

Cite this: *Chem. Sci.*, 2021, **12**, 9977

All publication charges for this article have been paid for by the Royal Society of Chemistry

Received 21st March 2021
Accepted 24th June 2021

DOI: 10.1039/d1sc01616d

rsc.li/chemical-science

A fluorescent probe for the discrimination of oxidation states of palladium†‡

Lijun Jiang, §[abc] Ho-Nam Mak, §[abc] Edward R. H. Walter, [a] Wing-Tak Wong,*[c] Ka-Leung Wong *[b] and Nicholas J. Long *[a]

Palladium-based catalysts are widely used in pharmaceutical industries, which can sometimes cause palladium contamination in pharmaceutical drug manufacture. It is important to separately quantify the different oxidation states of palladium (Pd^0 and Pd^{2+}) in pharmaceuticals as they react with scavengers differently. Although palladium sensors have been under intense investigation, oxidation state differentiators are very rare. Here, we report a simple porphyrin–coumarin conjugate, **PPIX-L2**, that can selectively discriminate between the oxidation states of palladium. The reaction of **PPIX-L2** with Pd^0 showed a 24-fold fluorescence increase of the coumarin emission, meanwhile, the presence of Pd^{2+} led to a 98% quenching of the porphyrin emission. Fluorescent responses of **PPIX-L2** towards Pd^0 and Pd^{2+} are specific, and its sensitivity towards both palladium species is significantly increased with a detection limit of 75 nM and 382 nM for Pd^0 and Pd^{2+} respectively.

Introduction

Palladium-catalysed reactions have become an indispensable tool in organic synthesis due to their strong ability and high efficiency in building versatile organic compounds.[1] This has realized a vast number of applications, not only in the research laboratory, but also in pharmaceutical industries.[2,3] In recent years, alternative non-precious metal-based catalysts including copper, nickel, and iron, have been developed.[4,5] However, palladium-based catalysts often offer significantly shorter routes towards the desired products due to their relatively higher activity in enabling the conversion of less reactive substrates, or at lower temperatures.[6,7] Shorter synthetic routes reduce the formation of side-products and waste, both of which are important points that have to be taken into account by pharmaceutical factories to minimize the plant costs.

However, when using 'precious metals' such as palladium for the production of pharmaceuticals, additional points have to be considered *e.g.* the possibility of contaminating the products with metal. Residual palladium in the body is highly toxic as it can bind to thiol-containing proteins or other biomacromolecules.[8–10] Usually, the amount of heavy metals in an active pharmaceutical ingredient has to be controlled to levels below 5–10 ppm.[11,12] If higher, specific scavengers are applied to remove the metal, thus substantial efforts are required to analyse residual metals. As Pd^0 and Pd^{2+} bind to scavengers differently,[12,13] it is necessary to separately detect and quantify the palladium species in active pharmaceutical ingredients.

Small molecule-based fluorescent probes are versatile tools which are frequently explored as metal sensors.[14–16] Although probes with novel structures or improved properties are routinely developed, it remains a very active research area. For example, two fluorescent rotaxane probes have been recently identified in Goldup's group as a selective Zn^{2+} and Pt^{2+} sensor.[17,18] As for palladium, there are also numerous probes designed for detecting Pd^0 (sometimes appeared as Pd^{2+} with reducing agents such as carbon monoxide and sodium borohydride)[19–25] or Pd^{2+}.[26–31] However, to the best of our knowledge, very few reports have described the discrimination of Pd^0 and Pd^{2+} within one fluorescent probe.[32,33] Koide's group developed an elegant fluorescein-constructed sensor to discriminate between Pd^0 and Pd^{2+} in a reaction-based manner in 2008.[32] Incubation of the sensor with Pd^0 and Pd^{2+} caused a fluorescence intensity increase at 526 nm and 535 nm respectively. The sensor is able to detect 10 ppm Pd^0, and its detection limit for Pd^{2+} was calculated as 3.9 μM. Although the maximum emission wavelength caused by Pd^0 and Pd^{2+} is different, specifically 526 nm by Pd^0 and 535 nm by Pd^{2+}, the 9 nm difference in the maximum wavelength is insignificant in the broad fluorescein emission, decreasing its sensitivity to discriminate Pd^0 and Pd^{2+}

[a]*Department of Chemistry, Imperial College London, MSRH Building, White City Campus, London, W12 0BZ, UK. E-mail: n.long@imperial.ac.uk*

[b]*Department of Chemistry, Hong Kong Baptist University, Kowloon Tong, Kowloon, Hong Kong SAR, China. E-mail: klwong@hkbu.edu.hk*

[c]*Department of Applied Biology and Chemical Technology, The Hong Kong Polytechnic University, Hung Hom, Kowloon, Hong Kong SAR, China. E-mail: w.t.wong@polyu.edu.hk*

† Dedication: For Professor Wolfgang Keim, an outstanding and inspirational scientist, on his 70th birthday.

‡ Electronic supplementary information (ESI) available: Details of synthesis, chemical structure characterization and photophysical measurement. See DOI: 10.1039/d1sc01616d

§ Authors with equal contribution.

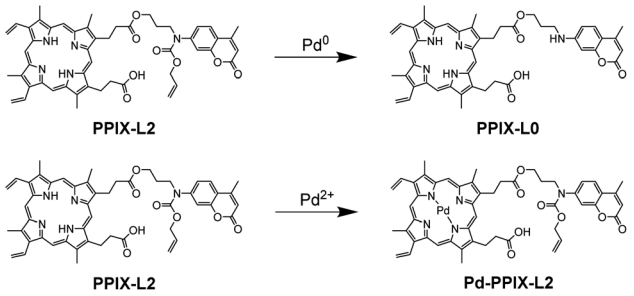

Fig. 1 Proposed detection strategy for Pd^0 and Pd^{2+}.

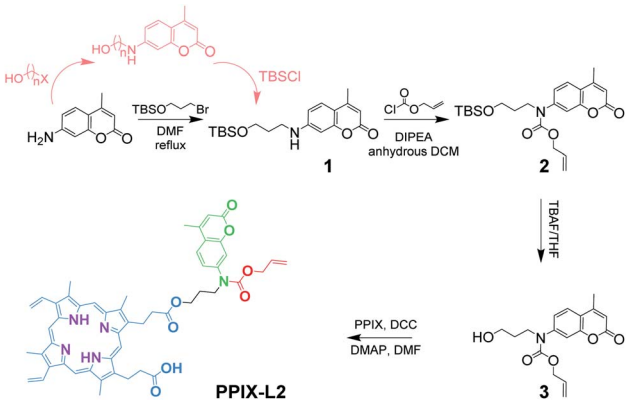

Scheme 1 Synthetic route and chemical structure of PPIX-L2.

in pharmaceutical drugs. A more recent example describing a non-reaction based colorimetric and anthraquinone-imidazole probe was reported by Kim and co-workers, where both Pd^0 and Pd^{2+} demonstrated a quenching effect on the emission of the probe, with a calculated detection limit of 2.84 μM and 1.65 μM respectively.[33] However, the discrimination between Pd^0 and Pd^{2+} relied on the colour change of the probe, which is hard to quantify. Higher concentrations of palladium species are also required for an observable readout (in the micromolar range), making it impractical for analysis of the oxidative states of Pd^0 and Pd^{2+} in active pharmaceutical ingredients, where concentrations are generally much lower.

Here we report an alternative strategy to differentiate between Pd^0 and Pd^{2+} by using a simple porphyrin–coumarin conjugate **PPIX-L2** (Fig. 1). Although porphyrins are known to bind metal ions, porphyrin derivatives have not been exploited as a probe for the discrimination of palladium species. The designed conjugate showed a significant increase of coumarin fluorescence at 440 nm and a quenching of porphyrin fluorescence at 631 nm towards Pd^0 and Pd^{2+} respectively. Changes in coumarin and porphyrin fluorescence caused by Pd^0 and Pd^{2+} are independent and have no interference on each other. **PPIX-L2** also demonstrated a much lower detection limit towards Pd^0 (75 nM) and Pd^{2+} (382 nM), which are as great as 38-fold and 10-fold lower, respectively, compared to the previously reported differentiators.

Results and discussion

Design and synthesis of PPIX-L2

The synthesis of **PPIX-L2** started from the substitution reaction of commercially available 7-amino-4-methylcoumarin and 3-bromo-1-propanol. The hydroxyl group in 3-bromo-1-propanol was first protected with *tert*-butyldimethylsilane (TBS), as it was found that it reacts with allyl chloroformate preferentially in the second step, due to the steric hindrance presented around the nitrogen atom in compound **1** (Scheme 1). Another route was also attempted towards the synthesis of **1**, by reacting 7-amino-4-methylcoumarin with a halogenated alcohol first (n = 2, 3; X = Cl, Br, I), followed by alcohol protection with TBSCl (presented in pink in Scheme 1). Here, it was found that the halogenated alcohol starting material underwent an intramolecular reaction under these conditions, forming an ether bond, and significantly decreasing the reaction yield of the desired product. The length of the carbon chain and halogen reactivities in the TBS-protected alcohol towards **1** were also investigated. The three-carbon chain showed a better reactivity compared to the two-carbon chain as it further decreased the electron donating effect from the oxygen to the halogen, and hence increased its reactivity. Bromide was shown to have a higher reactivity than chloride. Given these observations, (3-bromopropoxy)-*tert*-butyldimethylsilane was chosen, and the finalized synthetic route was determined shown in the black route of Scheme 1 (characterization data shown in Fig. S6–S16‡).

Distinctive fluorescence responses of PPIX-L2 to Pd^0 and Pd^{2+}

To study the behaviour of **PPIX-L2** as a responsive sensor for Pd^0, a fluorescence titration with $Pd(PPh_3)_4$ was conducted. To avoid Pd^0 oxidation, N_2 was bubbled through the solution during the measurements. The addition of Pd^0 to **PPIX-L2** in MeOH led to a gradual increase of the coumarin emission centred at 440 nm, as well the coumarin absorbance centred at around 353 nm, based on the well-studied Pd^0-catalyzed Tsuji–Trost reaction (λ_{ex}: 361 nm, Fig. 2a, S1 and S2‡).[19–25,34] Increase of the coumarin fluorescence is time-dependent, a bar graph describing changes of fluorescence intensity over time is shown in Fig. 2b. **PPIX-L2** was shown to quickly respond to Pd^0, displaying a 1.5-fold fluorescence increase immediately after the addition of Pd^0. A significant fluorescence increase can be observed in the first three hours, where the fourth hour displayed only a mild increase. A final 24-fold increase of the fluorescence intensity of **PPIX-L2** at 440 nm was caused by Pd^0. To verify the interaction of Pd^0 with **PPIX-L2** occurs through the Tsuji–Trost reaction mechanism, a MALDI-TOF mass analysis was performed for **PPIX-L2** upon Pd^0 addition. The product with expected mass of **PPIX-L0** was clearly shown in the mass spectrum, which confirmed the Pd^0 sensing mechanism (Fig. S3‡). In contrast, titrations of other investigated metal ions (M), including Pd^{2+}, revealed no change of the fluorescence spectra after 4 h (Fig. 2c).

Having confirmed the responsive increase in coumarin emission of **PPIX-L2** towards Pd^0, we extended our investigation of **PPIX-L2** to Pd^{2+} (Fig. 3, $PdCl_2$ was used as the source of Pd^{2+}).

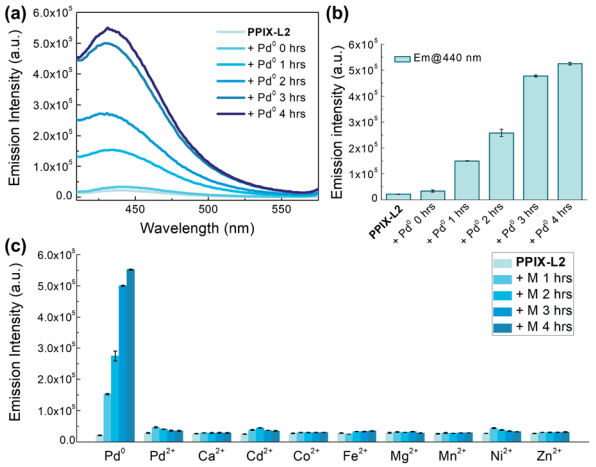

Fig. 2 Fluorescence profile of **PPIX-L2** (MeOH, 2 μM, $\lambda_{ex} = 361$ nm) to Pd^0. Changes of (a) fluorescence spectra, (b) coumarin fluorescence intensity at 440 nm of **PPIX-L2** on Pd^0 (10 μM) over time. (c) Metal selectivity. The selectivity of **PPIX-L2** to Pd^0. [M] = 10 μM. The *y*-axis is coumarin fluorescence intensity of **PPIX-L2** at 440 nm.

Addition of Pd^{2+} resulted in the striking decrease in porphyrin fluorescence of **PPIX-L2** and had no effect on the coumarin fluorophore (Fig. 3a). The decrease was determined to be time-dependent (Fig. 3b). The rapid decline of the porphyrin fluorescence up to 81% was seen immediately after the addition of Pd^{2+}, and plateaued at a time point of 1 h, with an almost total quenching of the porphyrin fluorescence presented. A further titration was performed, focusing on changes of porphyrin fluorescence in the first one hour following addition of Pd^{2+} (Fig. 3c), confirming the fast and efficient detection of Pd^{2+} by **PPIX-L2**. Pleasingly, all other metal ions produced no or a much smaller variation of the porphyrin fluorescence of **PPIX-L2** (Fig. 3d). As the porphyrin core can act as a cavity for different metal ions, a competition experiment was also performed (Fig. 3e). Pd^{2+} was shown to be able to displace metal ions from **PPIX-L2** in all cases; addition of M followed by Pd^{2+} to **PPIX-L2** led to a rapid and significant decrease of the porphyrin fluorescence. Thus, the porphyrin–coumarin system can serve as a simple and effective system for the discrimination of palladium species.

Improved detection limit of PPIX-L2 to Pd^0 and Pd^{2+}

Having identified **PPIX-L2** as a fluorescent differentiator for Pd^0 and Pd^{2+}, we then measured its detection limit towards the two palladium species. Correlations between fluorescence of **PPIX-L2** and concentrations of Pd^0/Pd^{2+} are demonstrated in Fig. 4. A linear relationship was observed in the concentration range of 0–1 μM at 2 hours after addition of Pd^0 and 0–4 μM at 1 hour after addition of Pd^{2+} (Fig. 4a and b). Using the 3σ method,[35] the detection limit towards Pd^0 and Pd^{2+} was determined as 75 nM and 382 nM respectively. Importantly, both values are much lower than the previously reported palladium species differentiators. Furthermore, we investigated the ability of **PPIX-L2** to quantify the concentration for Pd^0 and Pd^{2+} in one mixed sample. Therefore, a Pd^0 and Pd^{2+} mixed ion solution ([Pd^0] = 0.25 μM, [Pd^{2+}] = 2 μM) was prepared. The emission intensity of **PPIX-L2** with the mixed sample was recorded and used for the

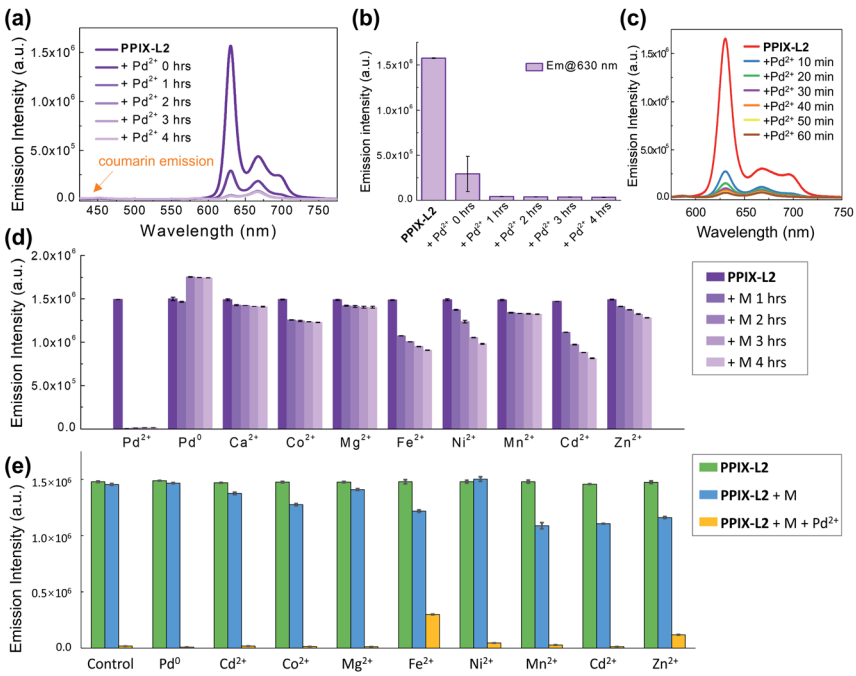

Fig. 3 Fluorescence profile of **PPIX-L2** (2 μM, MeOH, $\lambda_{ex} = 400$ nm) to Pd^{2+}. Changes of (a) fluorescence spectra, (b) porphyrin fluorescence intensity at 630 nm of **PPIX-L2** on Pd^{2+} (10 μM) over time. (c) Changes of porphyrin fluorescence spectra of **PPIX-L2** within the first one hour of the addition of Pd^{2+} (10 μM). (d) Metal selectivity and (e) Metal competitively (intensity was measured at 1 h after the addition of M/Pd^{2+}). [M/Pd^{2+}] = 10 μM. The *y*-axis is fluorescence intensity at 630 nm.

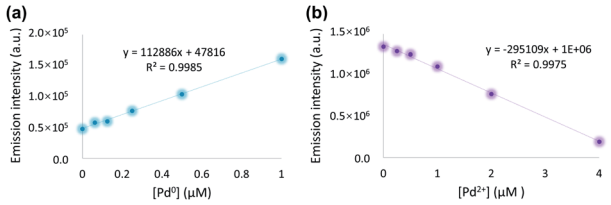

Fig. 4 Fluorescence analysis of PPIX-L2 against various concentrations of Pd^0 and Pd^{2+} in MeOH for the determination of detection limit. (a) Linear correlation between coumarin fluorescence intensity of 5 μM PPIX-L2 at 440 nm and [Pd^0]. Fluorescence intensity was recorded at 2 hours after the addition of Pd^0 (λ_{ex} = 361 nm). (b) Linear correlation between porphyrin fluorescence intensity of 2 μM PPIX-L2 at 631 nm and [Pd^{2+}]. Fluorescence intensity was recorded at 1 hour after the addition of Pd^{2+} (λ_{ex} = 400 nm).

calculations. The calculated concentration is 0.23 μM and 2.17 μM for Pd^0 and Pd^{2+} respectively (Table S1‡). Both values are having only 8% error to the actual concentration, suggesting **PPIX-L2** is able to quantitatively determine the two ions at the same time in one mixed sample solution. Besides, an additional detection limit measurement using the mixed sample solution was also conducted (Fig. S4‡). The detection limit for Pd^0 and Pd^{2+} under this condition was calculated as 97 nM and 390 nM respectively. Although both value increases a little bit compared to that in the single sample, it is still far lower than the previously reported differentiators.

Selectivity mechanism of PPIX-L2 to Pd^{2+}

To study the mechanism by which **PPIX-L2** possesses the high selectivity towards Pd^{2+}, a portion-wise titration of Pd^{2+} with a longer treatment time of 8 h to allow for a complete interaction, was performed and analyzed with the Stern–Volmer equation (Fig. 5).[36] The linear relationship between the relative fluorescence intensity of the probe under low concentrations of the quencher (Pd^{2+}), allows an easy graphical determination of Stern–Volmer quenching constant (K_{sv}), which defines the quenching efficiency. The linear relationship is shown in Fig. 5b, with the determined K_{sv} as 10^6 M^{-1}, demonstrating Pd^{2+} is an effective quencher of the porphyrin fluorescence of **PPIX-L2**. Double logarithmic of the Stern–Volmer plot further revealed the binding of **PPIX-L2** with Pd^{2+} is extremely strong, with a binding constant (K_b) of 1.41 × 10^7 M^{-1} calculated for a 1 : 1 binding stoichiometry. Therefore, the strong binding between Pd^{2+} and **PPIX-L2** is the likely underlying mechanism of the excellent selectivity of **PPIX-L2** towards Pd^{2+} (Fig. 5c). The binding of Pd^{2+} is likely to occur by coordinating with the four pyrrolic nitrogens in the porphyrin cavity. To corroborate this, an absorption titration with Pd^{2+} was conducted, given that metal-chelated porphyrin are more symmetrical with the production of a simplified Q band patterns to form only two Q bands (a spectral characteristic of porphyrin coordinated with a metal ion).[37] In particular for palladium(II) porphyrins, the two Q bands have been well described to appear at around 525 and 560 nm in the literature.[38–40] The absorption titration results are consistent with these descriptions, the four Q bands of **PPIX-L2** at 506, 540, 576 and 630 nm gradually diminished with a final appearance of only two Q bands at 519 and 555 nm (Fig. 5d). Furthermore, a MALDI-TOF analysis was performed to confirm the binding of the Pd^{2+} into the porphyrin cavity of **PPIX-L2** to form **Pd-PPIX-L2** with expected mass which matches the proposed detecting strategy (Fig. S5‡). These results demonstrate the formation of Pd^{2+}–porphyrin complex, suggesting the fluorescence decrease of **PPIX-L2** on Pd^{2+} is due to the heavy metal effect which leads to the phosphorescence emission.[41]

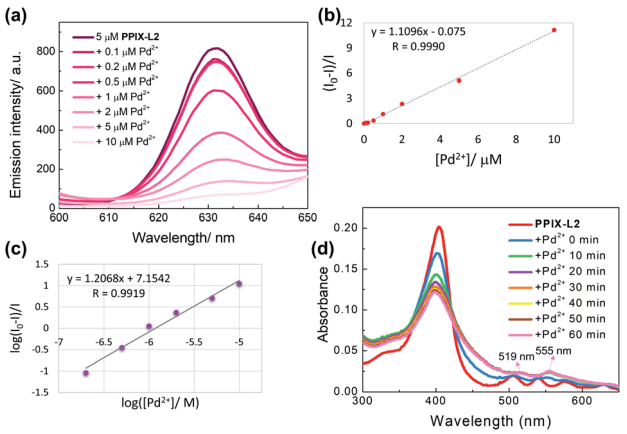

Fig. 5 Study of the interaction details of PPIX-L2 with Pd^{2+}. (a) Fluorescence profile of PPIX-L2 (5 μM) with various concentrations of Pd^{2+} (treatment time, 8 h). (b) Stern–Volmer analysis and (c) double logarithmic of the Stern–Volmer analysis of the decrease of fluorescence intensity at 631 nm on [Pd^{2+}]. (d) Absorption profile of PPIX-L2 (2 μM) on Pd^{2+} (10 μM) over time. Measurements were performed in MeOH.

Conclusions

In conclusion, we have identified a simple porphyrin–coumarin system **PPIX-L2** that can serve as an effective differentiator to discriminate the oxidation states of palladium (Pd^0 and Pd^{2+}) through the independent fluorescence changes of coumarin and porphyrin fluorophores, respectively. Importantly, we confirmed that **PPIX-L2** can impart not only the independent optical responses towards Pd^0 and Pd^{2+}, but also a degree of selectivity. Detection of Pd^0 by **PPIX-L2** is through the well-studied Tsuji–Trost reaction, therefore, the selectivity mechanism of **PPIX-L2** towards Pd^{2+} was examined in detail. Stern–Volmer analysis of the fluorescence titration results suggested that the strong binding between **PPIX-L2** and Pd^{2+} contributes to the selectivity. Absorption titration experiment and MALDI-TOF mass spectrum further confirms the formation of a Pd^{2+}–porphyrin complex. It is also noteworthy that **PPIX-L2** can demonstrate not only different optical responses towards Pd^0 and Pd^{2+}, but a much lower detection limit towards these palladium species (75 nM for Pd^0, 382 nM for Pd^{2+}) compared to the previously reported palladium differentiators. Crucially, the detection limit of **PPIX-L2** towards Pd^0 meets the requirement of palladium contamination set by European Agency. From a practical viewpoint, the next step is to further lower the detection limit of **PPIX-L2** for Pd^{2+}. Additionally, we are currently investigating the application of **PPIX-L2** in

pharmaceutical drugs to detect palladium contamination, especially the new chemical entities developed in the pharmaceutical industry. More generally, the results presented here demonstrate a new and simple system that can be exploited as effective palladium differentiators.

Data availability

Further details of the experimental procedures, photophysical measurements, and structural characterization are available in the ESI.

Author contributions

L. J., H. N. M., E. R. H. W., W.-T. W., K.-L. W. and N. J. L. designed the project. L. J. and H. N. M. carried out the synthesis and characterization of all samples. L. J. and H. N. M. performed photophysical measurements. L. J., H. N. M., W.-T. W., K.-L. W. and N. J. L. contributed new reagents and analyzed tools. L. J., H. N. M., W.-T. W., K.-L. W. and N. J. L. analyzed data. L. J., H. N. M., E. R. H. W. and N. J. L. wrote the paper. L. J., H. N. M., E. R. H. W., W.-T. W., K.-L. W. and N. J. L. discussed and commented on the manuscript.

Conflicts of interest

There are no conflicts to declare.

Acknowledgements

N. J. L. gratefully acknowledges the support of a Royal Society Wolfson Research Merit Award. K.-L. W. acknowledges the support from the Dr Mok Man Huang Endowed Professorship in HKBU Chemistry. We thank Dr P.-K. So (PolyU University Research Facility in Life Science) for technical assistance in MALDI-TOF mass spectrum. This work was supported by grants from Hong Kong Research Grant Council (HKBU 12300019).

Notes and references

1 A. Biffis, P. Centomo, A. Del Zotto and M. Zecca, *Chem. Rev.*, 2018, **118**, 2249–2295.
2 A. F. P. Biajoli, C. S. Schwalm, J. Limberger, T. S. Claudino and A. L. Monteiro, *J. Braz. Chem. Soc.*, 2014, **25**, 2186–2214.
3 A. O. King and N. Yasuda, in *Organometallics in Progress Chemistry*, Springer, Berlin, Heidelberg, 2017, pp. 205–245.
4 A. A. Gewirth, J. A. Varnell and A. M. Diascro, *Chem. Rev.*, 2018, **118**, 2313–2339.
5 G. A. Filonenko, R. Van Putten, E. J. M. Hensen and E. A. Pidko, *Chem. Soc. Rev.*, 2018, **47**, 1459–1483.
6 A. C. Frisch and M. Beller, *Angew. Chem., Int. Ed.*, 2005, **44**, 674–688.
7 Q. Xiao, S. Sarina, A. Bo, J. Jia, H. Liu, D. P. Arnold, Y. Huang, H. Wu and H. Zhu, *ACS Catal.*, 2014, **4**, 1725–1734.
8 T. Z. Liu, S. D. Lee and R. S. Bhatnagar, *Toxicol. Lett.*, 1979, **4**, 469–473.
9 C. Melber and I. Mangelsdorf, in *Palladium Emissions in the Environment: Analytical Methods, Environmental Assessment and Health Effects*, Springer Berlin Heidelberg, 2006, pp. 575–596.
10 J. Wataha, in *Encyclopedia of Metalloproteins*, Springer, New York, 2013, pp. 1628–1635.
11 J. S. Carey, D. Laffan, C. Thomson and M. T. Williams, *Org. Biomol. Chem.*, 2006, **4**, 2337–2347.
12 C. E. Garrett and K. Prasad, *Adv. Synth. Catal.*, 2004, **346**, 889–900.
13 H. Ren, C. A. Strulson, G. Humphrey, R. Xiang, G. Li, D. R. Gauthier and K. M. Maloney, *Green Chem.*, 2017, **19**, 4002–4006.
14 G. J. Stasiuk, F. Minuzzi, M. Sae-Heng, C. Rivas, H.-P. Juretschke, L. Piemonti, P. R. Allegrini, D. Laurent, A. R. Duckworth, A. Beeby, G. A. Rutter and N. J. Long, *Chem.–Eur. J.*, 2015, **21**, 5023–5033.
15 E. R. H. Walter, J. A. G. Williams and D. Parker, *Chem.–Eur. J.*, 2018, **24**, 7724–7733.
16 T. Hirayama, M. Inden, H. Tsuboi, M. Niwa, Y. Uchida, Y. Naka, I. Hozumi and H. Nagasawa, *Chem. Sci.*, 2019, **10**, 1514–1521.
17 M. Denis, J. Pancholi, K. Jobe, M. Watkinson and S. M. Goldup, *Angew. Chem., Int. Ed.*, 2018, **57**, 5310–5314.
18 Z. Zhang, G. J. Tizzard, J. A. G. Williams and S. M. Goldup, *Chem. Sci.*, 2020, **11**, 1839–1847.
19 F. Song, A. L. Garner and K. Koide, *J. Am. Chem. Soc.*, 2007, **129**, 12354–12355.
20 A. L. Garner and K. Koide, *Chem. Commun.*, 2009, 86–88.
21 J. Jiang, H. Jiang, W. Liu, X. Tang, X. Zhou, W. Liu and R. Liu, *Org. Lett.*, 2011, **13**, 4922–4925.
22 S. Pal, M. Mukherjee, B. Sen, S. K. Mandal, S. Lohar, P. Chattopadhyay and K. Dhara, *Chem. Commun.*, 2015, **51**, 4410–4413.
23 W. Feng, D. Liu, S. Feng and G. Feng, *Anal. Chem.*, 2016, **88**, 10648–10653.
24 Q. Wang, Q. Chen, C. Li, Q. Lai, F. Zou, F. Liang, G. Jiang and J. Wang, *Microchem. J.*, 2020, **153**, 1–5.
25 L. Lukomski, I. Pohorilets and K. Koide, *Org. Process Res. Dev.*, 2020, **24**, 85–95.
26 M. Santra, S. K. Ko, I. Shin and K. H. Ahn, *Chem. Commun.*, 2010, **46**, 3964–3966.
27 M. Wang, Y. Yuan, H. Wang and Z. Qin, *Analyst*, 2016, **141**, 832–835.
28 A. Kumar Bhanja, S. Mishra, K. Das Saha and C. Sinha, *Dalton Trans.*, 2017, **46**, 9245.
29 A. A. Soares-Paulino, L. Giroldo, N. A. Pradie, J. S. Reis, D. F. Back, A. A. C. Braga, H. A. Stefani, C. Lodeiro and A. A. Dos Santos, *Dyes Pigm.*, 2020, **179**, 108355.
30 X. Chen, Q. Ma, Z. Wang, Z. Xie, Y. Song, Y. Ma, Z. Yang and X. Zhao, *Asian J. Chem.*, 2020, **15**, 4104–4112.
31 H. Li, J. Fan and X. Peng, *Chem. Soc. Rev.*, 2013, **42**, 7943.
32 A. L. Garner and K. Koide, *J. Am. Chem. Soc.*, 2008, **130**, 16472–16473.
33 L. Rasheed, M. Yousuf, I. S. Youn, G. Shi and K. S. Kim, *RSC Adv.*, 2016, **6**, 60546–60549.

34 G. Hata, K. Takahashi and A. Miyake, *J. Chem. Soc., Chem. Commun.*, 1970, 1392–1393.
35 Title 40 – Protection of Environment: Code of Federal Regulations.
36 M. H. Gehlen, *J. Photochem. Photobiol., C*, 2020, **42**, 100338.
37 R. Giovannetti, *The Use of Spectrophotometry UV-Vis for the Study of Porphyrins*, 2012.
38 Q. X. Wan and Y. Liu, *Catal. Lett.*, 2009, **128**, 487–492.
39 S. Drouet, C. O. Paul-Roth, V. Fattori, M. Cocchi and J. A. G. Williams, *New J. Chem.*, 2011, **35**, 438–444.
40 Z. Valicsek and O. Horváth, *Microchem. J.*, 2013, **107**, 47–62.
41 L. Zang, H. Zhao, J. Hua, W. Cao, F. Qin, J. Yao, Y. Tian, Y. Zheng and Z. Zhang, *J. Mater. Chem. C*, 2016, **4**, 9581–9587.